

Two-particle correlations in continuum dipole transitions in Borromean nuclei

K. Hagino,¹ H. Sagawa,² T. Nakamura,³ and S. Shimoura⁴

¹ *Department of Physics, Tohoku University, Sendai, 980-8578, Japan*

² *Center for Mathematical Sciences, University of Aizu, Aizu-Wakamatsu, Fukushima 965-8560, Japan*

³ *Department of Physics, Tokyo Institute of Technology, 2-12-1 O-okayama, Tokyo 152-8551, Japan*

⁴ *Center for Nuclear Study, University of Tokyo (CNS) RIKEN Campus, 2-1 Hirosawa, Wako, Saitama 351-0198, Japan*

We discuss the energy and angular distributions of two emitted neutrons from the dipole excitation of typical weakly-bound Borromean nuclei, ^{11}Li and ^6He . To this end, we use a three-body model with a density dependent contact interaction between the valence neutrons. Our calculation indicates that the energy distributions for the valence neutrons are considerably different between the two nuclei, although they show similar strong dineutron correlations in the ground state to each other. This different behaviour of the energy distribution primarily reflects the interaction between the neutron and the core nucleus, rather than the interaction between the valence neutrons. That is, the difference can be attributed to the presence of s -wave virtual state in the neutron-core system in ^{11}Li , which is absent in ^6He . It is pointed out that the angular distribution for ^{11}Li in the low energy region shows a clear manifestation of the strong dineutron correlation, whereas the angular distribution for ^6He exhibits a strong anticorrelation effect.

PACS numbers: 21.10.Gv, 23.20.-g, 25.60.Gc, 27.20.+n

Borromean nuclei are unique three-body bound systems, in which any two-body subsystem is not bound [1, 2]. Typical examples include ^{11}Li and ^6He , which can be viewed as three-body systems consisting of a core nucleus and two valence neutrons. The binding energy of these neutron-rich nuclei is considerably small (the two-neutron separation energy, S_{2n} , is, 378 keV [3] and 975 keV for ^{11}Li and ^6He , respectively, which can be compared with *e.g.*, $S_{2n} = 12.2$ MeV for ^{18}O), and a few intriguing features originating from the weakly bound property have been found. A halo structure, in which the density distribution of valence neutrons extends far beyond the core nucleus [4, 5], and strong low-energy electric dipole ($E1$) transition [6, 7] are well-known examples.

One of the most important current open questions concerning the Borromean nuclei is to clarify the characteristic nature of correlations between the two valence neutrons, which do not form a bound state in the vacuum. A strong dineutron correlation, where the two neutrons take a spatially compact configuration, has been theoretically predicted for some time [1, 5, 8, 9, 10] (see also Refs. [11, 12]). It has been, however, a difficult task to probe experimentally the dineutron correlation. In fact, it is only recently when the strong low-lying dipole strength distribution has been observed experimentally in the ^{11}Li nucleus, which strongly suggests the existence of dineutron correlation in this nucleus.

A more direct information on the dineutron correlation may be obtained by measuring energy and angular distributions of two emitted neutrons [13, 14, 15]. Because neither ^{11}Li nor ^6He has a bound excited state, the Borromean nuclei have to be broken up to a three-body continuum state once they are excited as a result of the interaction with another nucleus. Notice that the operator which induces the $E1$ excitation is proportional to the center of mass coordinate of the two valence neu-

trons, $\mathbf{R} = (\mathbf{r}_1 + \mathbf{r}_2)/2$ [8, 16], where \mathbf{r}_1 and \mathbf{r}_2 are the coordinates for the two neutrons. Therefore, the relative motion of the two neutrons, $\mathbf{r} = \mathbf{r}_1 - \mathbf{r}_2$, is not affected by the $E1$ excitations at all. It is thus interesting to ask how the energy and angular distributions from the $E1$ excitation reflect the ground state properties of the Borromean nuclei, especially the correlation for the relative motion of the neutrons, that is, the dineutron correlation.

The aim of this paper is to address this question theoretically using a three-body model for the Borromean nuclei. The model which we employ is the same as that in Refs. [9, 17], that is, the three-body model with a density dependent zero-range pairing interaction between the two neutrons. The model predicts similar strong dineutron correlations for both the ^{11}Li and ^6He , although the spin structure of di-neutron is somewhat different from each other [9]. Furthermore, the model has successfully reproduced the experimental $E1$ strength distribution for both the nuclei [6, 18, 19]. Therefore, this three-body model provides a useful means to investigate the two-particle correlations in the dipole transitions in the ^{11}Li and ^6He nuclei. Moreover, by studying the two neutron correlations, one may also be able to shed some light on the Efimov effect [20], that is a general feature of a three-body system in which at least two of the three two-body subsystems have an infinite s -wave scattering length [21].

The energy and angular distributions based on the three-body model with a density dependent contact interaction have been computed by Esbensen and Bertsch in Ref. [16]. As all the basic formulas can be found there, we do not repeat them here. For the neutron-neutron and the neutron-core interactions, we use exactly the same parameters as those in Ref. [9], except for the radius parameter for the density dependent term in the pairing interaction for the ^{11}Li nucleus. We have slightly adjusted it so that the new empirical value of $S_{2n}=378\text{keV}$ [3] is reproduced. This yields the s -wave probability of

20.6% in the ground state of ^{11}Li . In order to calculate the continuum response, we treat approximately the recoil kinetic energy of the core nucleus for the three-body final state of the dipole response, although it is treated exactly for the initial (ground) state. That is, we ignore the off-diagonal component (the last term in Eq. (3.3) of Ref. [17]), whereas the diagonal term is included through the reduced mass [18, 19]. We have checked the accuracy of this approximation with the discretized dipole strength functions and have confirmed that the approximation works well both for ^{11}Li and ^6He [18].

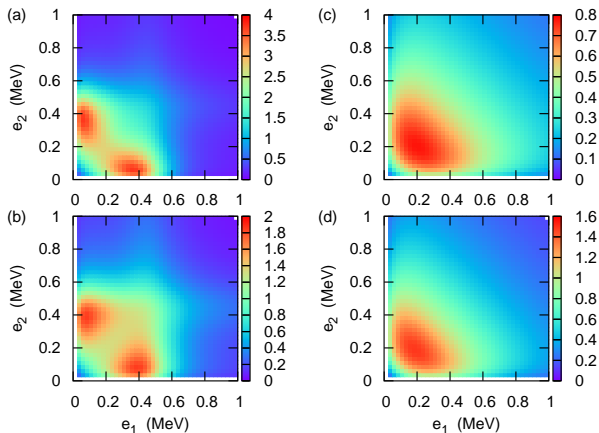


FIG. 1: (Color online) The dipole strength distributions, $d^2B(E1)/de_1de_2$, of ^{11}Li as a function of the energies of the two emitted neutrons relative to the core nucleus. They are plotted in units of $e^2\text{fm}^2/\text{MeV}^2$. Fig. 1(a) shows the correlated response, which fully takes into account the ground state and final state interactions between the two neutrons, while Fig. 1(b) shows the unperturbed response, obtained by neglecting the neutron-neutron interaction in the final states. Figs. 1(c) and 1(d) are obtained by assuming the plane-wave for the final states (*i.e.*, neglecting the neutron-core interaction) without and with the final state interaction between the two neutrons, respectively.

Figures 1 and 2 show the dipole strength distribution, $d^2B(E1)/de_1de_2$, as a function of the energies of the two emitted neutrons for the ^{11}Li and ^6He nuclei, respectively. Here, e_1 (e_2) is the relative energy between the first (second) neutron and the core nucleus. Notice that these energy distributions are symmetric with respect to the interchange of e_1 and e_2 . Fig. 1(a) shows the correlated response, which fully takes into account the final state interaction between the two neutrons, while Fig. 1(b) shows the unperturbed response, obtained by neglecting the neutron-neutron interaction in the final states. Figs. 1(c) and 1(d) are obtained by assuming the plane-wave for the final states (*i.e.*, neglecting the neutron-core interaction) without and with the final state interaction between the two neutrons, respectively. Figs. 2(a)-2(d) are the same, but for ^6He . All the calculations are performed by using the Green's function method [16].

One immediately notices that the strength distribution is considerably different between ^{11}Li and ^6He . For ^{11}Li , a large concentration of the strength appears at about $e_1=0.375$ MeV and $e_2=0.075$ MeV (and at $e_1=0.075$ MeV and $e_2=0.375$ MeV), with a small ridge at an energy of about 0.5 MeV. On the other hand, for ^6He , only a large ridge at about 0.7 MeV appears, and the strength is largely concentrated around $e_1 = e_2 = 0.7$ MeV. These features remain the same even if the final state interaction between the two emitted neutrons is switched off, as shown in Figs. 1(b) and 2(b), although the degree of the concentration of the strength is much more emphasized by the final state interaction. In contrast, if the interaction between the neutron and the core nucleus is neglected, the strength distribution is altered drastically, and in fact the distribution is now similar between the two nuclei (see Figs. 1(c), 1(d), 2(c), and 2(d)). Therefore, the different behaviours in the strength distribution should reflect primarily the property of the neutron-core interaction. In fact, the comparisons between Figs. 1(a) and 1(b), 1(c) and 1(d), 2(a) and 2(b), and 2(c) and 2(d) indicate that the final state neutron-neutron interaction does not play a major role in the shape of energy distribution.

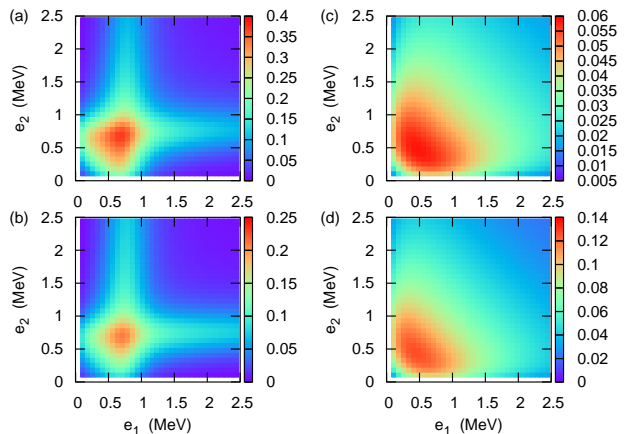


FIG. 2: (Color online) Same as Fig.1, but for ^6He .

The ridges in the strength function have already been discussed in the previous calculation for ^{11}Li by Esbensen and Bertsch [16]. They reflect the single-particle resonances, that is, the $p_{1/2}$ resonance around 0.54 MeV for ^{10}Li and the $p_{3/2}$ resonance at 0.91 MeV for ^5He [17]. These ridges correspond to the physical process in which one of the neutrons is excited by the dipole field while the other remains near the resonance state as a spectator in the neutron-core system [8, 16]. For ^{11}Li , in addition to the ridge, the dipole strength is concentrated in the region in which one of the neutrons has an energy close to zero. This reflects the s -wave virtual state in ^{11}Li close to zero energy [17, 20, 22, 23]. This virtual state is characterized by a large negative scattering length of

$a = -30_{-31}^{+12}$ fm [13] for the $n+{}^9\text{Li}$ system. In contrast, the s -wave scattering length is $a = 4.97 \pm 0.12$ fm [24] for the $n+{}^4\text{He}$ system, and the virtual state does not exist in ${}^5\text{He}$. Notice that the virtual state was not taken into account in the previous calculation for the dipole response of ${}^{11}\text{Li}$, and the concentration of the strength in the region of $e \sim 0$ was not found in Ref. [16].

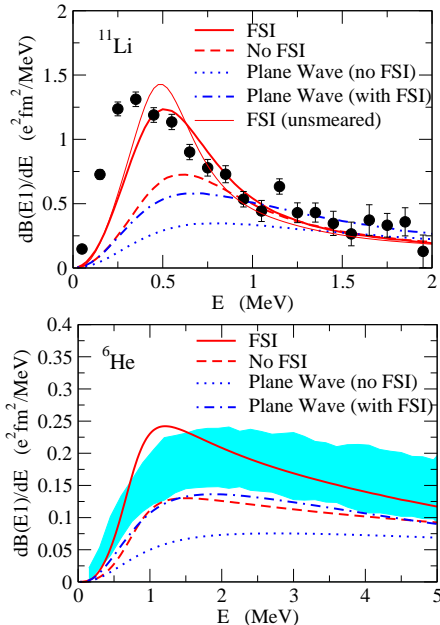


FIG. 3: (Color online) The upper panel: The dipole strength distribution for ${}^{11}\text{Li}$ as a function of $E = e_1 + e_2$. The thick solid, dashed, dotted, and dot-dashed lines are obtained under the same assumptions for Figs. 1(a), 1(b), 1(c), and 1(d), respectively. These curves are smeared with the experimental energy resolution. The thin solid line is the same as the thick solid line, but without the smearing. The experimental data are taken from [6]. The lower panel: the same as the upper panel, but for ${}^6\text{He}$. The shaded area shows the experimental data, taken from Ref. [7].

The dipole strength distribution for ${}^{11}\text{Li}$ at a fixed total energy of around $E = e_1 + e_2 = 0.45$ MeV has two distinguished peaks, one at $e_1/E \sim 0$ and the other at $e_1/E \sim 1$. It has been argued that the two peaked structure in the energy distribution is a characteristic feature of the Efimov effect [20]. It is a peculiar three-body effect for a system in which two or three two-body subsystems have a large scattering length. In ${}^{11}\text{Li}$, this condition is approximately fulfilled, as the scattering length is large and negative both for the nn and the n -core systems. In our calculation, the s -wave scattering length is -5.6 fm [17] for the n - ${}^9\text{Li}$ and $+2.43$ fm for the n - ${}^4\text{He}$ systems, where as it is -15 fm for the n - n system[17].

The dipole strength distributions,

$$\frac{dB(E1)}{dE} = \int de_1 de_2 \frac{d^2 B(E1)}{de_1 de_2} \delta(E - e_1 - e_2), \quad (1)$$

are plotted in Fig. 3. The solid, dashed, dotted, and dot-dashed lines are obtained under the same assumptions

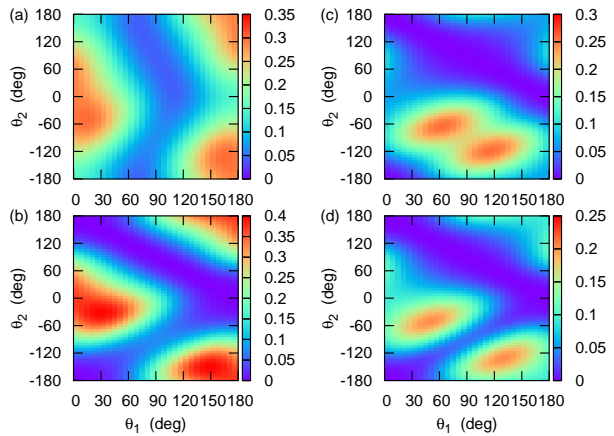


FIG. 4: (Color online) Angular distributions of the two valence neutrons in ${}^{11}\text{Li}$ and ${}^6\text{He}$ emitted in the rest frame of the corresponding nuclei. These are calculated for the configuration in which the two neutrons are emitted in the same reaction plane (*i.e.*, $\phi_1 = \phi_2$) by the longitudinal component of the E1 operator. Fig. 4(a) shows the angular distribution for ${}^{11}\text{Li}$ at $e_1 = 0.375$ MeV and $e_2 = 0.075$ MeV, while Figs. 4(b) and 4(c) are for $e_1 = e_2 = 0.225$ MeV and $e_1 = e_2 = 0.5$ MeV, respectively. Fig. 4(d) shows the angular distribution for ${}^6\text{He}$ at $e_1 = e_2 = 0.7$ MeV.

for Figs. 1(a)/2(a), 1(b)/2(b), 1(c)/2(c), and 1(d)/2(d), respectively. These curves are smeared with the experimental energy resolution [6]. Also shown by the thin solid line in Fig. 3(a) is the same as the thick solid line, but without the smearing. The experimental B(E1) distribution for ${}^{11}\text{Li}$ is obtained from the experimental breakup cross sections in Ref.[6], using $S_{2n} = 378$ keV. Because of the large concentration of the strength in the low energy region in the energy distribution shown in Fig. 1, the strength distribution for ${}^{11}\text{Li}$ has a significantly sharper peak as compared to that for ${}^6\text{He}$. Notice again that the strength distributions are qualitatively similar between the two nuclei if the dineutron correlation is neglected (see the dotted and the dot-dashed lines).

In order to discuss how the dineutron correlation in the ground state affects the dipole response, let us next consider the angular distributions of the two emitted neutrons. Figure 4 shows the angular distributions corresponding to the longitudinal component of the dipole excitation of the ${}^{11}\text{Li}$ and ${}^6\text{He}$ nuclei (induced by the $\mu = 0$ component of the E1 operator, $\hat{T}_{\lambda=1, \mu=0}$), that is, $\sum_{h_1, h_2} |f_{h_1 h_2}^{10}(\hat{\mathbf{k}}_1, \hat{\mathbf{k}}_2)|^2$, where h and $\hat{\mathbf{k}} = (\theta, \phi)$ are the helicity and the direction of the momentum vector for an emitted neutron, respectively. Here, $f_{h_1 h_2}^{1\mu}(\hat{\mathbf{k}}_1, \hat{\mathbf{k}}_2)$ is the amplitude of dipole excitation calculated with two-particle wave functions in the continuum state with definite momenta \mathbf{k}_1 and \mathbf{k}_2 and definite spins, where the momenta are defined in the rest frame of ${}^{11}\text{Li}$ and ${}^6\text{He}$ (see Eq. (5.5) in Ref. [16]).

The angular distribution for ${}^{11}\text{Li}$ for the energy at

which the dipole strength is concentrated, that is, $e_1 = 0.375$ MeV and $e_2 = 0.075$ MeV (see Fig. 1), is shown in Fig. 4 (a). The distribution is calculated for the configurations in which the two emitted neutrons are in the same reaction plane, that is, $\phi_1 = \phi_2$. Here the second neutron mainly occupies the s -wave virtual state, and the angular distribution for this neutron is widely spread. The energy and angular distributions are mainly determined by the virtual state for this energy configuration, and the effect of final state interaction does not seem to play a major role, as one can infer from Fig. 1. We have confirmed this by switching off the final state interaction in our calculation. We have in fact obtained a qualitatively similar angular distribution as in Fig. 4 (a).

The angular distribution for the same total energy $e_1 + e_2 = 0.45$ MeV as in Fig. 4(a), but for $e_1 = e_2 = 0.225$ MeV, is plotted in Fig. 4 (b). For this configuration, both the neutrons are emitted along the z axis (*i.e.*, $\theta_1 = \theta_2 = 0$) with a large probability, although the distribution is rather flat around $\theta_1 = \theta_2 = 0$, with the maximum at $\theta_1 = -\theta_2 = 30^\circ$. Therefore, the opening angle between the two neutrons is relatively small, and one would naively consider that the shape of this distribution strongly reflects the dineutron correlation, with some perturbation by the anticorrelation effect for the dipole excitation. As noted in Ref. [16], the anticorrelation, with which the two neutrons are emitted on opposite sides of the z axis, is associated with the projection of the wave function with a coherent mixture of s and d wave states onto the momentum states.

The anticorrelation is more pronounced at higher energies. Fig. 4 (c) shows the angular distribution at $e_1 = e_2 = 0.5$ MeV, which corresponds to the region of the ridge in the energy distribution shown in Fig. 1. For this energy configuration, the probability for emission of two neutrons on the same sides of the z axis (in the region of $\theta_2 > 0$) is largely suppressed, and the maximum of the distribution appears around $\theta_1 = 60^\circ$ and $\theta_2 = -66^\circ$.

Notice that the shape of the distribution is similar to the results of the previous calculation shown in Figs. 9 and 10 in Ref. [16]. The shape is determined by a destructive interference between the $[d \otimes p]$ and $[p \otimes s]$ configurations [16], excited from the $[p^2]$ and $[s^2]$ configurations in the ground state wave function. Therefore, the angular distribution around this energy is strongly affected by the p -wave single particle resonance. In fact, for the ${}^6\text{He}$ nucleus, where the energy distribution is characterized by the $p_{3/2}$ resonance, we obtain a very similar angular distribution at $e_1 = e_2 = 0.7$ MeV (see Fig. 4(d)). For ${}^6\text{He}$, it would therefore not be straightforward to probe the dineutron correlation in the ground state solely by the angular distribution, in which the dineutron correlation is largely masked by the effect of the p wave single particle resonance.

In summary, we have carried out the three-body model calculations for ${}^{11}\text{Li}$ and ${}^6\text{He}$ nuclei in order to investigate the energy and angular distributions of the two emitted neutrons from E1 excitations. We have shown that these distributions are strongly affected by the properties of the neutron-core potential, rather than the ground state properties. For the ${}^{11}\text{Li}$ nucleus, the presence of s -wave virtual state helps to reveal a clear manifestation of the strong dineutron correlation through the energy and the angular distributions. For the ${}^6\text{He}$ nucleus, on the other hand, it is not straightforward to probe it, due to the anticorrelation effect in the angular distribution. The correlation measurements for ${}^{11}\text{Li}$ have been recently done at RIKEN. The present calculations shown in this paper are qualitatively in good agreement with the preliminary data. We will report the analyses of these data in a separate paper.

We thank P. Schuck for useful discussions. This work was supported by the Japanese Ministry of Education, Culture, Sports, Science and Technology by Grant-in-Aid for Scientific Research under the program numbers (C) 20540277 and 19740115.

-
- [1] M.V. Zhukov *et al.*, Phys. Rep. **231**, 151 (1993).
[2] A.S. Jensen *et al.*, Rev. Mod. Phys. **76**, 215 (2004).
[3] C. Bachelet *et al.*, Phys. Rev. Lett. **100**, 182501 (2008).
[4] I. Tanihata *et al.*, Phys. Rev. Lett. **55**, 2676(1985).
[5] P.G. Hansen and B. Jonson, Europhys. Lett. **4**, 409 (1987).
[6] T. Nakamura *et al.*, Phys. Rev. Lett. **96**, 252502 (2006).
[7] T. Aumann *et al.*, Phys. Rev. **C59**, 1252 (1999).
[8] G.F. Bertsch and H. Esbensen, Ann. Phys. (N.Y.) **209**, 327 (1991).
[9] K. Hagino and H. Sagawa, Phys. Rev. **C72**, 044321 (2005).
[10] K. Hagino, H. Sagawa, J. Carbonell, and P. Schuck, Phys. Rev. Lett. **99**, 022506 (2007).
[11] M. Matsuo, K. Mizuyama, and Y. Serizawa, Phys. Rev. **C71**, 064326 (2005).
[12] N. Pillet, N. Sandulescu, and P. Schuck, Phys. Rev. **C76**, 024310 (2007).
[13] H. Simon *et al.*, Nucl. Phys. **A791**, 267 (2007); Few-Body Systems **43**, 199 (2008).
[14] L.V. Chulkov *et al.*, Nucl. Phys. **A759**, 23 (2005).
[15] F.M. Marqués *et al.*, Phys. Rev. **C64**, 061301(R) (2001).
[16] H. Esbensen and G.F. Bertsch, Nucl. Phys. **A542**, 310 (1992).
[17] H. Esbensen, G.F. Bertsch and K. Hencken, Phys. Rev. **C56**, 3054 (1997).
[18] K. Hagino and H. Sagawa, **C76**, 047302 (2007).
[19] H. Esbensen *et al.*, Phys. Rev. **C76**, 024302 (2007).
[20] E. Garrido, D.V. Fedorov, and A.S. Jensen, Phys. Rev. Lett. **96**, 112501 (2006).
[21] V.M. Efimov, Phys. Lett. **B33**, 563 (1970).
[22] B.M. Young *et al.*, Phys. Rev. **C49**, 279 (1994).
[23] I.J. Thompson and M.V. Zhukov, Phys. Rev. **C49**, 1904 (1994).
[24] R.A. Arndt *et al.*, Nucl. Phys. **A209**, 429 (1973).